

Selection of Time-after-injection in Bone Scanning using Compartmental Observers

Fernando Tadeo and Mustapha Ait Rami *

Abstract—An approach to assist the determination of the best time-after-injection for taking an scintigram in bone scanning is proposed. More precisely, a technique is discussed to estimate the evolution of the portions, in different compartments of the body, of the injected dose using a model of the radionuclide distribution dynamics, the available measurements and information on variations of the parameters. At each time, the possible range of variation of these unmeasured states is evaluated, and from this the expected evolution of the contrast of the image is obtained. This makes it possible to predict the best time for taking the image. To show the applicability, a practical example is provided.

Keywords: Observers, Compartmental models, Medical engineering, Bone scanning

1 Introduction

Bone scanning is a method for examining pathologies (specially skeletal ones) that uses a large gamma camera to pick up the radioactivity produced by a radioactive substance (radionuclide) previously injected into the bloodstream [1]. The result is an image, called a scintigram, like the one shown in Figure 1, that helps to detect and characterize pathologies such as bone neoplasms or osteomyelitis.

This paper proposes a method to deal with a difficulty in scintigrams: deciding when is the best time for the scan, after injection. Although rules-of-thumbs exist, this time is normally selected from experience [1]. For an image point of view, the best time corresponds to the instant when there is maximum contrast in the image between the 'hot spots' (areas with pathology) and the background. As it is normally impractical to obtain images continuously, an approach is proposed in this paper based on mathematical tools to predict this contrast, to aid the physician carrying out the procedure to select the most adequate time. These mathematical tools are

based on using a compartmental model of the radionuclide diffusion in the body (more precisely, the one in [2], which has been extensively validated in clinical trials), combined with a recent proposal on observers, by the authors [3, 4], which gives a simple methodology for estimating bounds of unmeasured variables. A preliminary result was provided in [5], based on continuously measuring the concentration in blood of the radionuclide, which is not adequate in practice. In this paper, we further develop those results, concentrating on the procedure to make implementation of the approach in clinical practice feasible, by using a few measurements of the concentration in blood of the radionuclide.

For illustration, kinetic models of the bone-seeking radiopharmaceutical Tc-MDP in adult humans are used to show that, by using the proposed approach, it is possible to predict the evolution of the contrast that can be obtained in the scintigram. This is based on providing estimations of the unmeasured variables, giving upper and lower bounds on the portions of dose in different parts of the body. Note that the proposed approach is general, as it is based on compartmental models [6], so it is applicable to other problems in medicine and biology, such as those in [7, 8, 9].

2 Bone scanning

The procedure for taking an scintigram is the following: the patient receives an injection of a radionuclide, which, transported by the blood, collects in the bones. More of it tends to collect in so-called 'hot spots', areas where there is increased metabolic activity (which in simple terms means that the bone is breaking down, or repairing itself). The gamma rays generated by the radionuclide are captured by a specific camera, that provides the image [1].

Several radionuclides are used: Calcium analogues (such as Strontium 85 and 87), hydroxyl group analogues (Fluorine 18) and Phosphonate Analogues (Methylen Dyphosphonate and M. Hydroxydiphosphonate). This paper concentrates on the use of Dyphosphonates, more precisely Tc-99m(Sn)Methylene Diphosphonate, as it is the most commonly used due to its rapid bone uptake and

*The authors are with Dpt. of Systems Engineering and Automatic Control, University of Valladolid, 47005 Valladolid, Spain. Tel: +34 983423566 Email: {fernando,aitrami}@autom.uva.es. This work is funded by project DPI2007-66718-C04-02. Dr. Ait Rami is funded by a "Ramón y Cajal" grant from MiCInn.



Figure 1: Example of scintigram

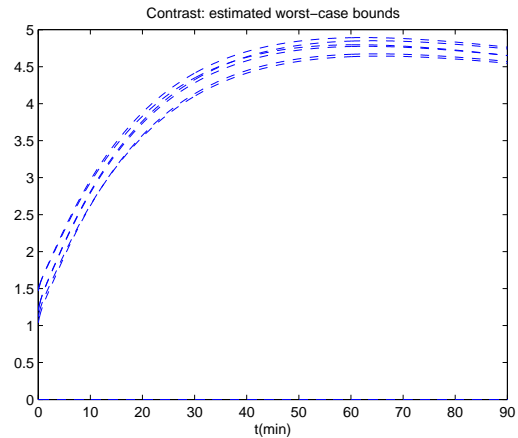


Figure 2: Evolution of the contrast in the image for several virtual patients

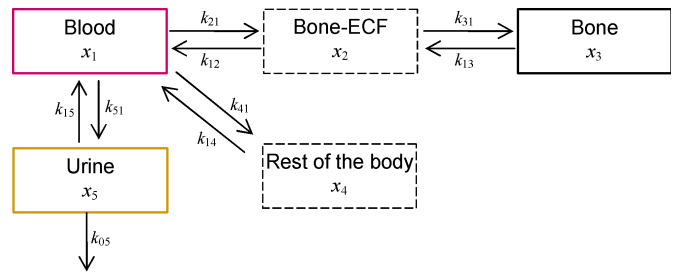


Figure 3: Compartmental model for radionuclide distribution in the body

urinary clearance (within 3 hours almost half of the dose is already in the bone, and most of the rest is already cleared through the kidneys).

Deciding when is the adequate time-after-injection for the scan is tricky: From a purely imaging point of view, the optimal time is the instant when the maximum contrast in the image between the 'hot spots' and the background is obtained. Unfortunately, the evolution of the contrast of the scintigram varies intra-patient, as can be seen in Figure 2, which plots the evolution of the contrast of the image for several models of patients.

This paper develops an approach based on estimating this contrast (in fact tight bounds on it) from the simulation of a mathematical model of the uptaking process. In particular, this is done using the model derived in [2], where the kinetics in adult humans of Tc-99m(Sn)Methylene Diphosphonate (Tc-MDP) were studied for bone scanning. Based on clinical measurements, the portion of the administered dose of this radionuclide in some compartments of the human body was determined to be quite

precisely given by the following dynamical model:

$$\frac{dx}{dt} = \begin{bmatrix} -k_{21} - k_{41} - k_{51} & k_{12} & 0 & k_{14} & k_{15} \\ k_{21} & -k_{12} - k_{32} & k_{23} & 0 & 0 \\ 0 & k_{32} & -k_{23} & 0 & 0 \\ k_{41} & 0 & 0 & -k_{14} & 0 \\ k_{51} & 0 & 0 & 0 & -k_{15} - k_{05} \end{bmatrix} x(t),$$

$$y(t) = [c \ 0 \ 0 \ 0 \ 0] x(t), \quad (1)$$

where the column vector $x(t)$ contains the states, that correspond to the portion of the dose of Tc-MDP in the different compartments: $x_1(t)$ is the portion of the dose in the blood, $x_2(t)$ in the extracellular fluid of the bone, $x_3(t)$ in cellular bone, $x_5(t)$ in the tubular urine and $x_4(t)$ in the rest of the body (see Figure 3 for a diagram of the compartmental model). Some values for the parameters of the model were obtained from physiological data. Based on clinical measurements [2], the following parameters for the compartmental model (1) were obtained, with some uncertainty that represents inter-patient variations: $k_{12} = 0.540 \pm 0.038$, $k_{21} = 0.095 \pm 0.003$, $k_{14} = 0.277 \pm 0.007$, $k_{41} = 0.431 \pm 0.011$, $k_{15} = 0.233$, $k_{51} = 0.024$, $k_{05} = 0.749$, $k_{23} = 0.049 \pm 0.001$, and $k_{32} = 1.055 \pm 0.037$. It can be seen that there is a significant inter-patient variation of parameters.

Our objective is to provide a technique that uses the mathematical model provided, and the available information on the parameters, to design an observer that, at each time, gives upper and lower bounds on the portions of dose in different parts of the body. The estimations will be updated, using discontinuous measurements of the dose in the blood.

3 Proposed Bounding Observer

The mathematical methodology used in this paper to get tight estimations of the evolution of the portion of dosing in each of the compartments of the body is based on the general procedure presented by the authors in [3, 4]. This procedure makes it possible to estimate states for compartmental systems, always ensuring that the estimated states are logical (i.e., never negative), providing tight bounds on the estimated variables, and taking into account uncertain parameters and initial states. Thus, the *compartmental observation problem*, which consists of constructing compartmental observers [10], is studied: observers that ensure the compartmental properties of the states (i.e., positivity and conservation). We must point out that although methodologies to include information on uncertainty are available [11, 12, 13, 14], unfortunately, they are quite complex. On the contrary, the proposed approach is simple to apply and does not need involved calculations.

This methodology is based on the fact that compartmental systems like the one in Figure 3 can always be mathematically described by the following dynamic system:

$$\frac{dx}{dt} = Ax(t), \quad y(t) = Cx(t). \quad (2)$$

That is, the system whose states are to be estimated on-line can be described as a system with p measured variables (that form the column vector $y(t)$) and n internal states (that describe the portion of dose in each compartment, and form the state vector $x(t)$). Thus, the square constant matrix A is composed of $n \times n$ elements (that will be denoted a_{ij}), and the constant matrix C has n rows and p columns of elements, denoted c_{ij} . It is assumed that bounds on the initial state are known: $\underline{x} \leq x(0) \leq \bar{x}$, and the matrices A and C have some uncertainty, but they can be bounded by matrices $\underline{A}, \bar{A}, \underline{C}$ and \bar{C} , such that

$$\underline{A} \leq A \leq \bar{A} \text{ and } \underline{C} \leq C \leq \bar{C}.$$

The proposed approach is based on using an observer with two independent sets of states: one set (denoted $\bar{\Theta}$) is used to derive an upper bound on the real value, whereas a complementary set ($\underline{\Theta}$) makes it possible to derive a lower bound.

The proposed observer is then given by the following two independent dynamical equations:

$$\frac{d\bar{\Theta}}{dt} = (\bar{A} - L\underline{C})\bar{\Theta}(t) + L\bar{y}(t), \quad \frac{d\underline{\Theta}}{dt} = (\underline{A} - L\bar{C})\underline{\Theta}(t) + L\underline{y}(t). \quad (3)$$

Bounds on the states are then estimated by integrating (3), starting from adequate initial conditions.

For the designer of the observer, a central aspect is the selection of the observer gain L , that must be selected to a bounding observer, so it must fulfill certain mathematical conditions, discussed in [4, 5].

When there are only a few measurements available, the outputs $\underline{y}(t)$ and $\bar{y}(t)$ can be estimated as follows: the lower bound $\underline{y}(t)$ is given by

$$\begin{aligned} \underline{y}(t) &= y(t) \text{ if a measurement of } y(t) \text{ is available,} \\ &= \underline{\Theta}(t) \text{ otherwise.} \end{aligned} \quad (4)$$

whereas for the lower bound:

$$\begin{aligned} \bar{y}(t) &= y(t) \text{ if a measurement of } y(t) \text{ is available,} \\ &= \bar{\Theta}(t) \text{ otherwise.} \end{aligned} \quad (5)$$

That is, each time a measured output is available, that output is immediately used in the observer. Otherwise, the corresponding bounds are used as estimations of the output.

4 Proposed solution for determining time-after-injection

The previous section presented a methodology to estimate portions of dose in different compartments of the body using compartmental models, by integrating the dynamical equations 3. To apply this methodology to the bone scanning problem it is necessary to define the observer matrices $\underline{A}, \bar{A}, \underline{C}, \bar{C}$ L and the initial conditions, which is done in this section.

To define matrices \underline{A} and \bar{A} , we can directly use clinical measurements, such as those of [2] presented in Section 2. This gives directly the following matrices, that bound the state matrix of the compartmental model:

$$\underline{A} = \begin{bmatrix} -0.541 & 0.502 & 0 & 0.270 & 0.233 \\ 0.092 & -1.520 & 0.048 & 0 & 0 \\ 0.0 & 1.018 & -0.048 & 0 & 0 \\ 0.420 & 0 & 0 & -0.270 & 0 \\ 0.024 & 0 & 0 & 0 & -0.982 \end{bmatrix}, \quad (6)$$

$$\bar{A} = \begin{bmatrix} -0.584 & 0.578 & 0 & 0.284 & 0.233 \\ 0.098 & -1.670 & 0.050 & 0 & 0 \\ 0.020 & 1.092 & -0.050 & 0 & 0 \\ 0.442 & 0 & 0 & -0.284 & 0 \\ 0.024 & 0 & 0 & 0 & -0.982 \end{bmatrix}. \quad (7)$$

Regarding the bounds on matrix C , if blood measurements are used, taking into account the tolerance δ on

the measurements, the bounds on this output matrix are:

$$\underline{C} = [1 - \delta \quad 0 \quad 0 \quad 0 \quad 0], \quad (8)$$

$$\overline{C} = [1 + \delta \quad 0 \quad 0 \quad 0 \quad 0]. \quad (9)$$

Following the methodology in [5], the following observer gain that ensures that a bounding observer can be selected:

$$L = \begin{bmatrix} 12 \\ 0.0365 \\ 0.005 \\ 0.335 \\ 0.024 \end{bmatrix}. \quad (10)$$

The proposed compartmental observer (3), with this gain, can be used to provide upper and lower bounds on the portion of dose in the different compartments of the model, taking into account also the unavoidable uncertainty in the system parameters and initial conditions. These initial conditions of the system, when the observation starts (simultaneously with the injection of the radionuclide), can be bounded within the following range:

$$\begin{bmatrix} 1 - \delta \\ 0 \\ 0 \\ 0 \\ 0 \end{bmatrix} \leq x(0) \leq \begin{bmatrix} 1 + \delta \\ 0.03 \\ 0.03 \\ 0.01 \\ 0.01 \end{bmatrix}, \quad (11)$$

where the small factors δ take into account the unmodulated blood diffusion and transportation dynamics and the fact that the first measurement might not be exactly simultaneous with the injection.

Thus, to get correct bounds, the initial condition of the lower observer states is just

$$\underline{\varrho}(0) = [1 - \delta \quad 0 \quad 0 \quad 0 \quad 0]^T, \quad (12)$$

whereas the initial condition of the upper states is

$$\overline{\varrho}(0) = [1 + \delta \quad 0.03 \quad 0.03 \quad 0.01 \quad 0.01]^T. \quad (13)$$

Using the proposed observer with the parameters discussed in this section, the evolution of the portion of dose in each of the compartments $x(t)$ will always be between the estimated states $\underline{\varrho}(t)$ and $\overline{\varrho}(t)$. Moreover, these bounds are tight, and are always nonnegative.

Once bounds on the states are available, it is not difficult to estimate bounds on the expected contrast of the scintigram. For example, we define the *target* Q_T and *background* Q_B to be

$$Q_T = x_3 + x_2 + 0.1x_1, \quad Q_B = x_4 + 0.9x_1,$$

which makes it possible to derive bounds on the *contrast*, defined by

$$\text{contrast} = \frac{Q_T}{Q_B}.$$

These bounds are then:

$$\overline{\text{contrast}} = \frac{\overline{\varrho}_3 + \overline{\varrho}_2 + 0.1\overline{\varrho}_1}{\overline{\varrho}_4 + 0.9\overline{\varrho}_1},$$

$$\underline{\text{contrast}} = \frac{\underline{\varrho}_3 + \underline{\varrho}_2 + 0.1\underline{\varrho}_1}{\underline{\varrho}_4 + 0.9\underline{\varrho}_1}. \quad (14)$$

5 Example of application

This section present the application of the methodology discussed in previous section to several ‘virtual patients’. Thus, the derivation of bounds application is based on first integrating the dynamical equations (3), starting from the initial conditions (13), and where the observer matrices are given by (7)-(9), and then deriving the bounds on the contrast using (14).

The ‘virtual patients’, correspond to computer simulations of the compartmental model (1), for the parameters obtained for the patients in the original study. The results for those patients showed that the proposed procedure worked correctly, making it possible to obtain tight bounds on the states.

For example, Figures 4 to 8 plot the evolutions of the portion of dose in different parts of the body, for one of these ‘virtual patients’, together with the bounds estimated using the approach proposed in Section 3, that uses measurements of the concentration in blood of the radionuclide at times 0 and 10 minutes (a detail of the evolution of the dose in bone-ECF is shown in Figure 9, to clarify the rapid uptaking of the radionuclide by the bone-ECF). To make the results reproducible, it was assumed in this experiment that there are no significant variations of the system parameters throughout the experiment. In all the plots the bounds on the states obtained with the proposed approach are nonnegative and converge to the real values, giving lower and upper bounds on the real states that converge to the real values.

Using these estimations, an evolution of the figures of merits used to derive imaging times can be directly calculated. In this case the objective is to distinguish in the images the bone from the surrounding tissue. Using the proposed definition for the contrast of the scintigram, the evolution of the bounds is depicted in Figure 10.

The evolution of states and contrast agrees well with the clinical practice [15, 16, 17].

6 Conclusions

This paper proposed a new approach to assist the determination of the best time-after-injection for taking a scintigram in bone scanning. The technique is based on transforming the problem into an observation prob-

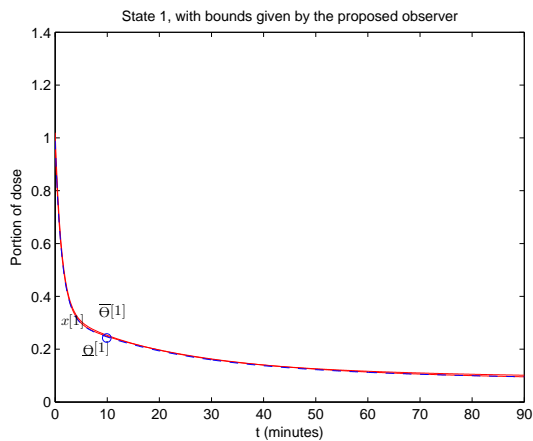


Figure 4: Evolution of concentration in blood, and estimated bounds

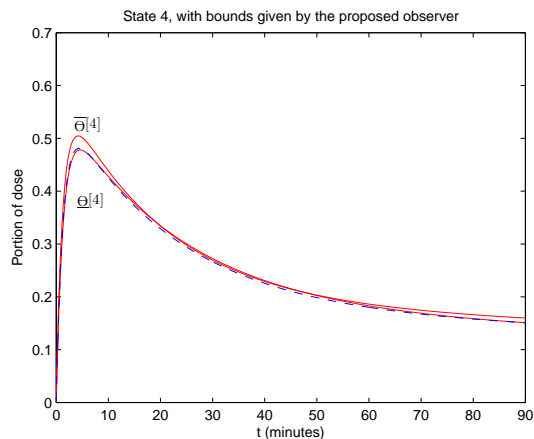


Figure 7: Evolution of concentration in non-bone-ECF for virtual patient, and estimated bounds

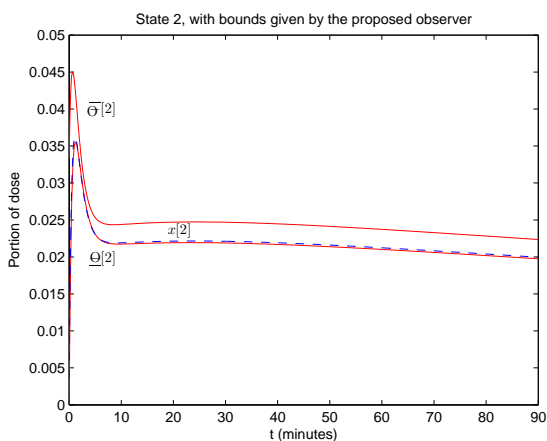


Figure 5: Evolution of concentration in bone-ECF for virtual patient, and estimated bounds

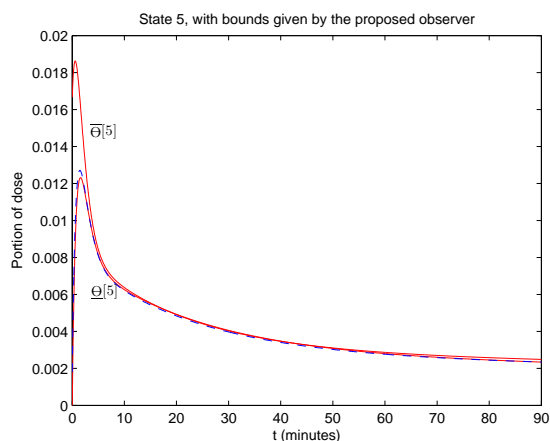


Figure 8: Evolution of concentration in urine for virtual patient, and estimated bounds

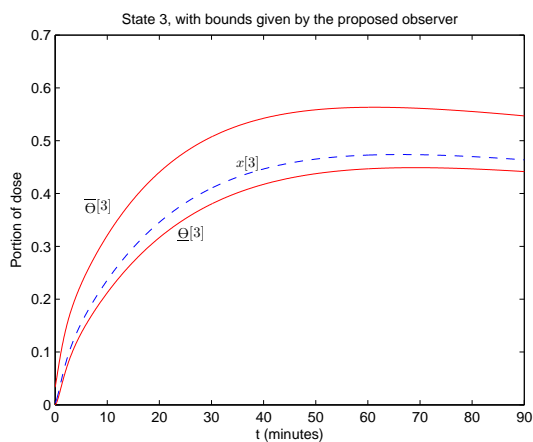


Figure 6: Evolution of concentration in bone for virtual patient, and estimated bounds

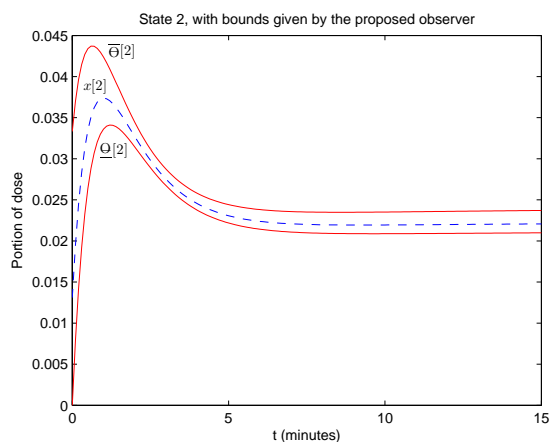


Figure 9: Detail of Figure 5

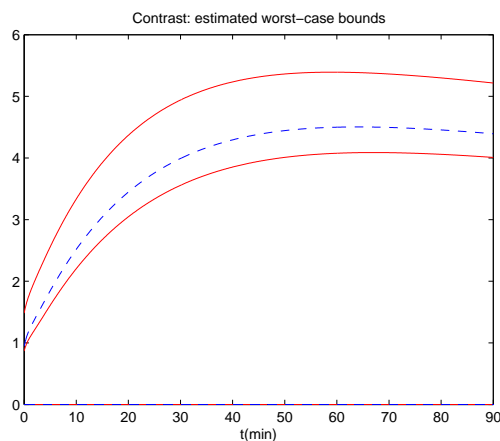


Figure 10: Evolution of the contrast for the virtual patient, and estimated bounds

lem for compartmental models, so that techniques proposed by the authors to provide upper and lower bounds on unmeasured states can be used. An illustrative case study, based on the use of Tc-99m(Sn)methylene diphosphonate, shows the feasibility of the proposed approach, and how it can be used to provide tight estimations of the concentration of radionuclide in the different compartments of the body, and as a consequence, makes it possible to predict the contrast.

References

- [1] Fogelman, I., *Bone Scanning in Clinical Practice*, Springer Verlag, London, 1987.
- [2] Makler, P.T., Charkes, N.D., "Studies of Skeletal Tracer Kinetics IV. Optimum Time Delay for Tc-99m(Sn) Methylene Disphosphonate Bone Imaging," *J Nucl Med*, 21: 641-645, 1980.
- [3] Ait Rami, M., Helmke, U., Tadeo, F., "Positive Observation Problem For Linear Time-Lag Positive Systems". *IFAC Workshop on Systems, Structure & Control*, Foz de Iguazu, Brazil, 2007.
- [4] Ait Rami, M., Helmke, U., Tadeo, F., "Positive observation problem for time-delays linear positive systems", *IEEE Mediterranean Control Conference*, Greece, 2007.
- [5] Tadeo, F., Ait Rami, M., "Observation with Bounds of Biological Systems: A Linear Programming Approach," in *Positive Systems (Ed.: Bru & Romero-Vivo)*, Springer Verlag, 2009.
- [6] Jacquez, J.A., *Compartmental Analysis in Biology and Medicine*, Ann Arbor, MI: Univ. of Michigan Press, 1985.
- [7] Hynne, F., Dano, S., Sorensen, P.G., "Full-scale model of glycolysis in *Saccharomyces cerevisiae*," *Biophysical Chemistry*, 94: 12116, 2001.
- [8] Luzyanina, T., Mrusek, S., Edwards, J.T., Roose, D., Ehl, S., Bocharov G., "Computational analysis of CFSE proliferation assay," *J Math Biology* 54(1): 57-89, 2007.
- [9] Linninger, A.A., Xenos, M., Sweetman, B., Ponkshe, S., Guo, X., Penn, R., "A mathematical model of blood, cerebrospinal fluid and brain dynamics," *J Math Biology*, 59(6): 729-759, 2009.
- [10] Van Den Hof, J.M., "Positive linear observers for linear compartmental systems". *SIAM J on Control & Optimization*, 36: 590-608, 1998.
- [11] Gouze, J.L., Rapaport, A., Hadj-Sadok, Z.M., "Interval observers for uncertain biological systems," *J Ecological Modelling*, 133:45-56, 2000.
- [12] Combastel, C., "A state bounding observer for uncertain nonlinear continuous-time systems based on zonotopes," *IEEE Conf on Decision and Control*, Seville, Spain, 2005.
- [13] Rapaport, A., Dochain, D., "Interval observers for biochemical processes with uncertain kinetics and inputs," *Mathematical Biosciences*, 193(2): 235-253, 2005.
- [14] Alamo, T., Bravo, J.M., Camacho, E.F., "Guaranteed state estimation by zonotopes," *Automatica*, 41(6): 1035-1043, 2005.
- [15] Subramanian, G., McAfee, J.G., Blair, R.J., et al., "An evaluation of Tc-99m labeled phosphate compounds as bone imaging agents," *Radiopharmaceuticals*, 319-328, 1975.
- [16] Rosenthal, L., Arzoumanian, A., Lisbona, R., et al., "A longitudinal comparison of the kinetics of Tc-99m MDP and Tc-99m EHDP in humans," *Clin Nucl Med*, 2: 232-234, 1997.
- [17] Fogelman, I., Citrin, D.L., McKillop, J.H., et al., "A clinical comparison of Tc-99m HEDP and Tc-99m MDP in the detection of bone metastases," *J Nucl Med*, 20: 98-101, 1979.